Max-Planck-Institut für Meteorologie

REPORT No. 49

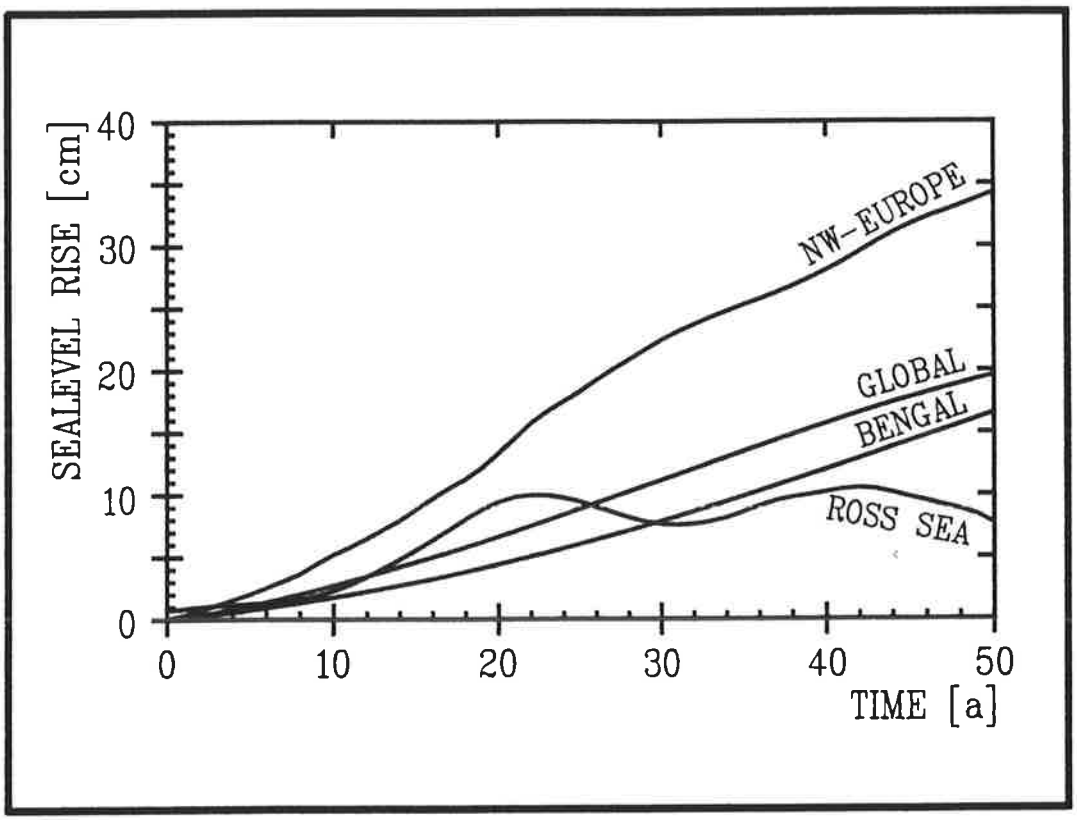

OCEAN RESPONSE TO GREENHOUSE WARMING

by

U. MIKOLAJEWICZ • B. SANTER • E. MAIER-REIMER

HAMBURG, MARCH 1990

AUTHORS:

UWE MIKOLAJEWICZ — MAX-PLANCK-INSTITUT FUER METEOROLOGIE

BENJAMIN SANTER — MAX-PLANCK-INSTITUT FUER METEOROLOGIE

ERNST MAIER-REIMER — MAX-PLANCK-INSTITUT FUER METEOROLOGIE

MAX-PLANCK-INSTITUT
FUER METEOROLOGIE
BUNDESSTRASSE 55
D-2000 HAMBURG 13
F.R. GERMANY

Tel.: (040) 4 11 73-0
Telex: 211092
Telemail: MPI.Meteorology
Telefax: (040) 4 11 73-298

ISSN 0937–1060

Ocean Response to Greenhouse Warming

Uwe Mikolajewicz, Benjamin Santer and Ernst Maier-Reimer

Max-Planck Institut für Meteorologie
Bundesstrasse 55
D-2000 Hamburg 13
F. R. Germany

Abstract

An ocean general circulation model is used to simulate the sea level change resulting from a rapid greenhouse warming. The changes in sea level and sea surface temperature are regionally strongly variable. The projected global mean sea level rise due to thermal expansion alone is 19 cm in 50 years. However, regional values can vary between 40 cm and even a decrease in sea level due to changes in ocean circulation. The simulated oceanic change patterns are compared with measurements.

1 Introduction

An increase in sea level is likely to be a first order impact of greenhouse-gas-induced climate change. Even moderate changes in sea level (less than 50 cm) can have tremendous societal and economic impacts, particularly in heavily-populated regions of the world which are close to sea level. Projecting regional changes in sea level is therefore extremely important.

Several recent studies have considered the transient response of coupled ocean-atmosphere models to time-dependent CO_2 and greenhouse-gas forcing (1,2,3), but have not discussed sea level changes. Virtually all studies which have examined the sea level response have used simple 1-D pure diffusive or upwelling-diffusive models (4,5) in which only thermal expansion is treated. These investigations cannot simulate the regional distribution of sea level change. The only study which has attempted to do this, including both thermal expansion and extremely simplified ocean dynamics, yielded spatially homogenous sea level changes (6). Here we consider both thermal effects and the full dynamic effects associated with changes in oceanic general circulation.

In the present study we isolate the purely oceanic response to a 'pseudo-transient' atmospheric forcing consisting of monthly mean surface air temperature anomalies ($2xCO_2$ minus $1xCO_2$) derived from atmospheric general circulation model (AGCM) equilibrium response experiments. We examine the robustness of certain features of the coupled models' oceanic response (such as inter-hemispheric asymmetry in the sea surface temperature (SST) changes) in a simpler uncou-

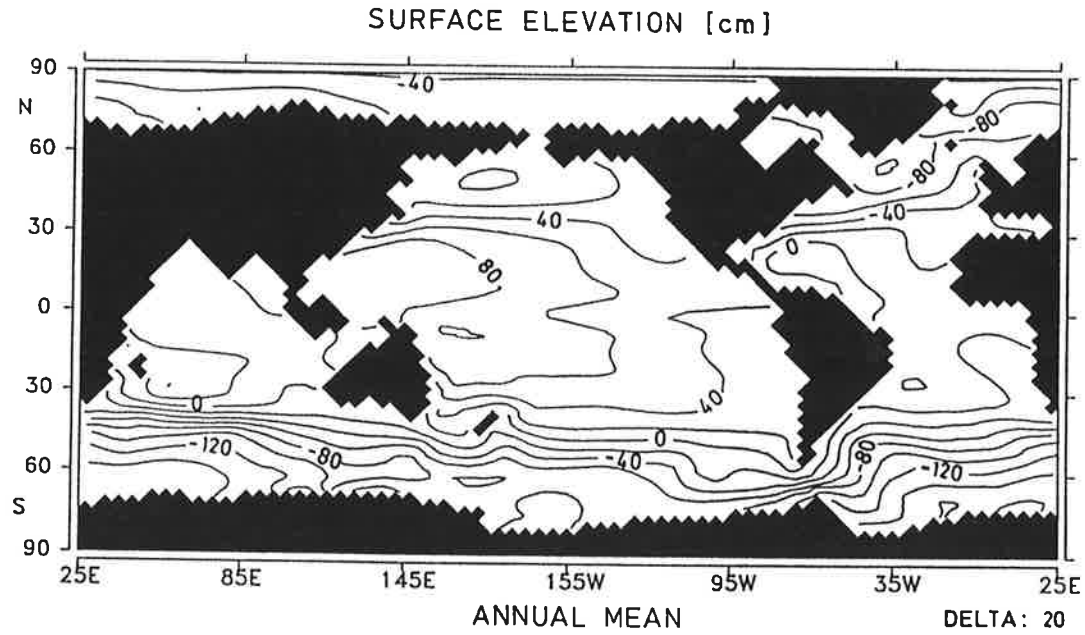

Figure 1a: Annual mean distribution of sea surface elevation of the control experiment.

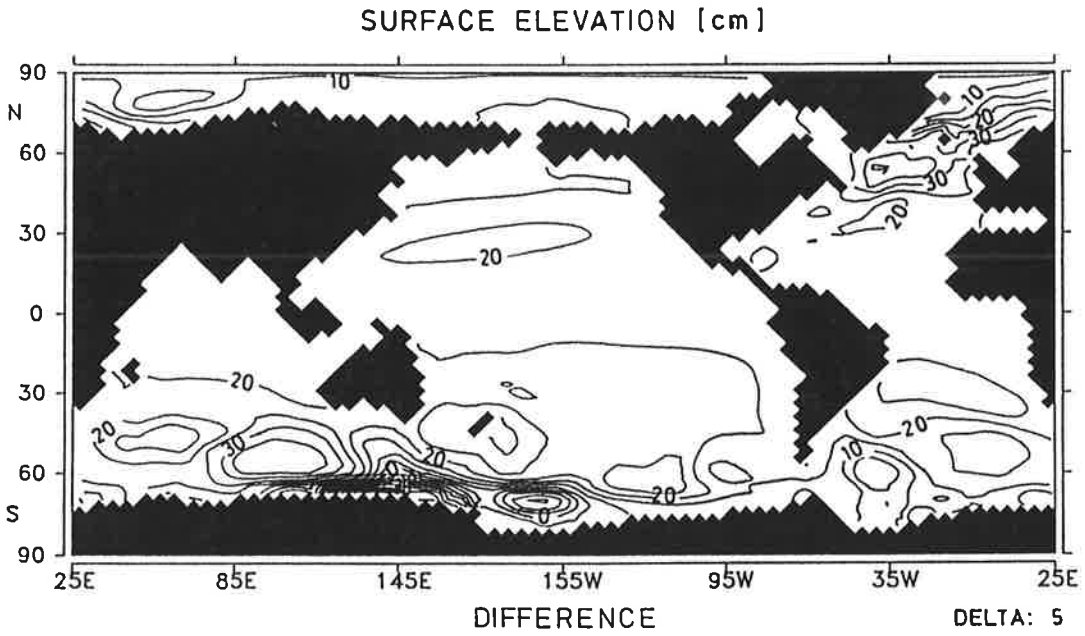

Figure 1b: Pattern of changes in sea surface elevation for year 50 relative to the control experiment. Note that changes in the Ross Sea area are negative.

pled experiment using an ocean general circulation model (OGCM) with realistic thermohaline circulation.

2 The model

We use the Hamburg large-scale-geostrophic OGCM (7). The model is based on the conservation laws for heat, salt and momentum (the latter in a linearized form) and uses the hydrostatic assumption. The flow field is divided into a vertically-averaged barotropic component and the residual baroclinic components. The model has a dynamically active sea surface elevation. Changes in the surface elevation are due to divergence of flow, thermal expansion and fresh water fluxes. The formulation of the model is fully implicit, so that a time step of 30 days can be used, as compared with a few hours typical for explicit integration schemes. A one-layer thermodynamic sea ice model with advection is included.

The horizontal resolution is 3.5 x 3.5 degrees on an E-type grid (8). The model has 11 vertical layers (centered at 25, 75, 150, 250, 450, 700, 1000, 2000, 3000, 4000 and 5000 m).

The model was spun up from an initially homogeneous state and integrated for 10000 years to steady state with climatological forcing (monthly mean wind stress (9) and air temperature (10) and annual mean climatological surface salinity (11)) coupled to the top layer with Newtonian time constants of approximately 2 months. During the last 500 years of spin up the fresh water fluxes required to restore the salinity to climatology were stored and used as forcing in a control run, for which the surface salinity was no longer prescribed but computed from the fresh water fluxes. Initially the model showed a slight drift with this type of forcing, but after a further 4000 years of integration the model again reached a steady state which was very close to the state attained before switching to fresh water flux forcing.

The model exhibits a realistic mean thermohaline circulation (12) with a flow of 17 Sverdrup (10 tons/sec) of North Atlantic deep water (NADW) leaving the Atlantic at 30°S to the Southern Ocean. At 24°N the strength of the meridional overturning is 20 Sverdrup compared to 17 Sverdrup derived from observations (13). The strength of the Antarctic Circumpolar current (ACC) is 122 Sverdrup, compared to 123 Sverdrup ±10 from pressure gauge measurements (14). The annual mean sea surface elevation of the control run is displayed in figure 1a, showing the well-known subtropical gyres and the ACC. The equilibrium circulation fields attained after this procedure were used as initial conditions for the following experiment.

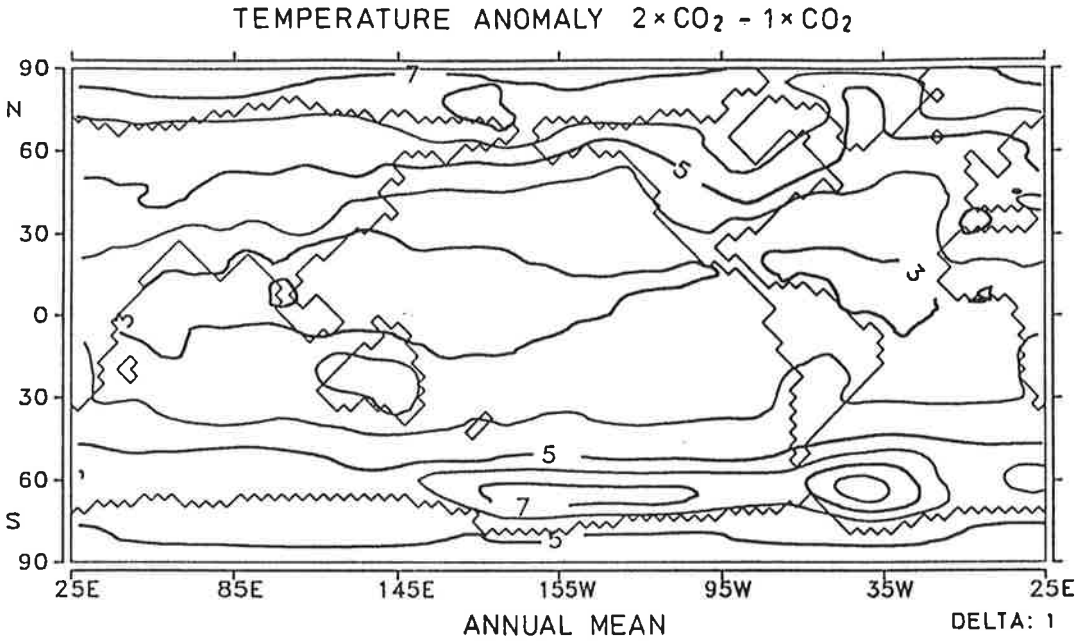

Figure 2a: Pattern of annual mean "model average" surface air temperature anomaly used as forcing for the simulation. The global mean of this temperature anomaly is 4°C (computed over ocean points only). For sources of model data see text.

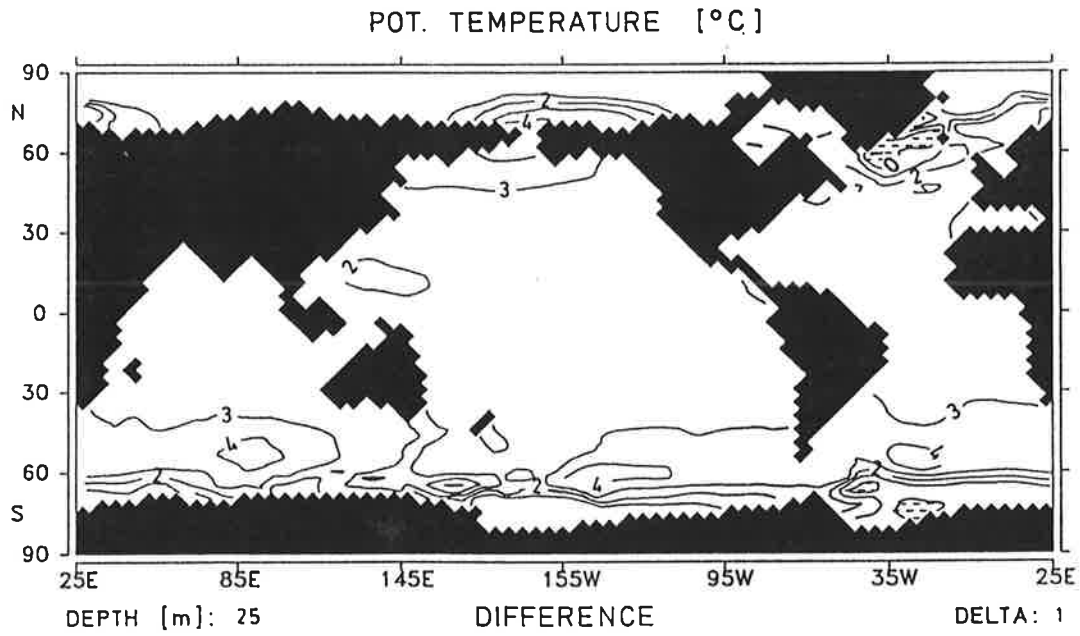

Figure 2b: Geographical distribution of changes in SST in year 50 relative to the control experiment. Shading indicates negative values.

3 The experiment

The ocean model was driven by monthly mean surface air temperature anomalies ($2xCO_2$ minus $1xCO_2$) derived from four equilibrium response experiments conducted with the Goddard Institute for Space Studies (GISS), Geophysical Fluid Dynamics Laboratory (GFDL), Oregon State University (OSU) and United Kingdom Meteorological Office (UKMO) AGCMs (15,16,17,18). All AGCMs were coupled with mixed-layer oceans. Rather than using results from a single model only, surface air temperature changes for the four models were interpolated to the OGCM grid and averaged. The resulting model average anomaly fields, defined as an annual cycle over 12 months, utilize all published equilibrium response results from models with comparable levels of atmosphere-ocean interaction, except for results from the National Center for Atmospheric Research (NCAR; 19), which were not available.

The patterns of $2xCO_2$ minus $1xCO_2$ surface temperature changes were very similar for the four models, with poleward amplification of the temperature change in the winter hemisphere due to ice-albedo feedback effects. The major inter-model differences were in the amplitudes of the surface temperature changes. Thus our averaging procedure should not significantly smooth the response patterns while being less biased by individual model sensitivities. The averaged monthly mean anomaly fields were positive everywhere with a mean warming of 4°C over the oceans. The annual mean spatial pattern of the applied temperature anomaly is shown in figure 2a.

We assumed that the model-average patterns are time-invariant, only the amplitude varying during the transition from $1xCO_2$ to $2xCO_2$. To simulate the expected transient temperature increase in response to time-dependent greenhouse-gas forcing, the amplitude evolution was described by the linear exponential function $f(t) = 1 - e^{-(t-t_0)/a}$ with a time constant $a = 40$ years. The initial time t_0 was set to January 1st for year 0. The time evolution of the mean forcing temperature changes over the oceans is shown in figure 3a; by the year 50 the projected warming is 2.9°C. The forcing due to possible changes in the wind stress and fresh water fluxes relative to the control run was not considered.

The neglect of atmospheric feedback, anomalous wind stress and fresh water flux forcing, and the assumption of time-invariant patterns of the surface temperature change in the forcing fields clearly represent major idealizations in our experimental design. Recent evidence from the few GCM experiments which have been performed with time-dependent greenhouse-gas forcing suggests in fact that important differences may exist between the equilibrium and transient response patterns (1,3,20). We stress that the experiment performed here must be regarded only as a zeroth order test of the sensitivity of the ocean circulation to a specified forcing, and not a prediction. However, we feel that such a test can give valuable insight into typical sea level response properties which may not have been generally appreciated and which would also apply to a more realistic coupled ocean-atmosphere

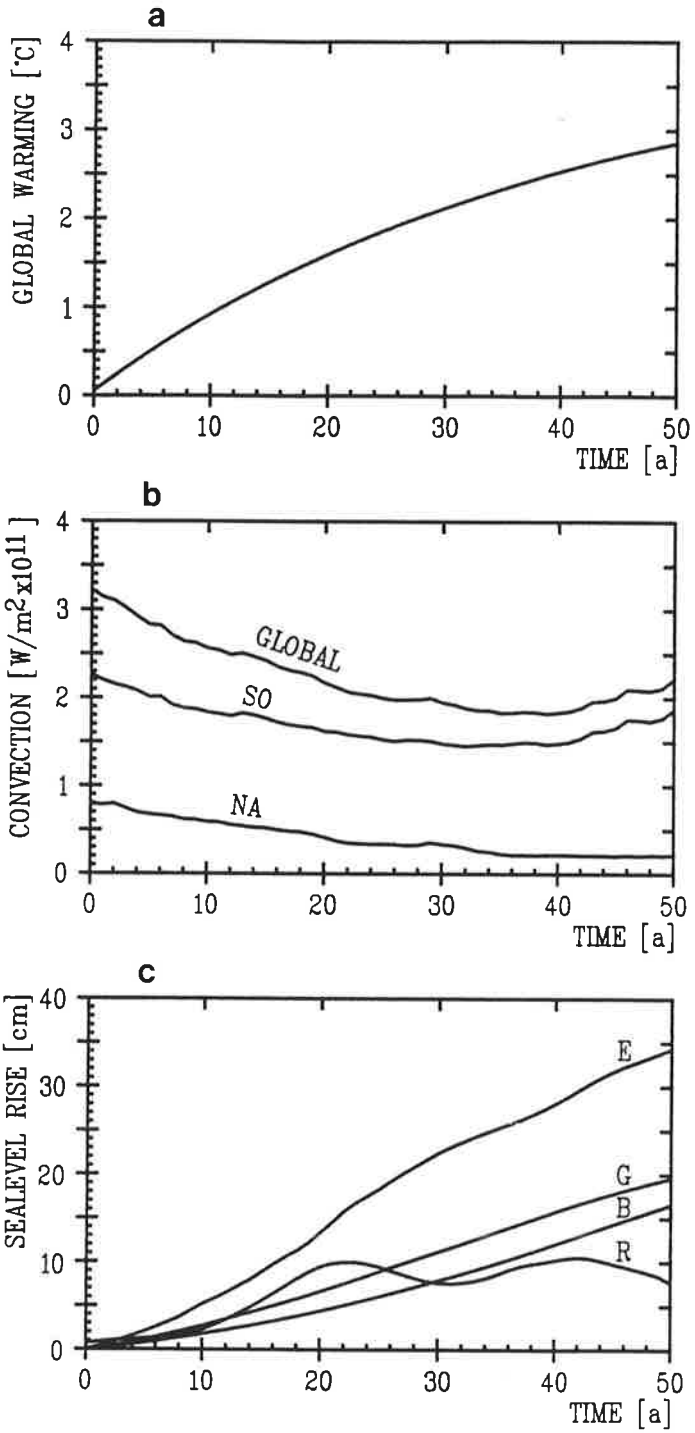

Figure 3a: Time evolution of annual mean globally averaged surface air temperature anomaly imposed on the OGCM.

Figure 3b: Time evolution of global, North Atlantic (NA) and Southern Ocean (SO) deep water formation, measured as rate of loss of potential energy due to convection.

Figure 3c: Sea level rise as a function of time: global mean (G), North West Europe (E), Ross Sea (R) and Bay of Bengal (B).

simulation.

4 Results

The time evolution of the deep water production (measured as the rate of loss of potential energy by convection) is shown in figure 3b. The global deep water production decreases initially and attains a minimum in year 40 (approximately 2/3 of its original value). The fractional reduction is stronger in the North Atlantic than in the Southern Ocean. After the year 40, the global deep water formation increases again. This can be attributed exclusively to increased formation of Antarctic Bottom water (AABW). Generally there is a trend in the deep water formation to a higher fraction of AABW compared to NADW.

Figure 2b displays the changes in SST for the year 50 relative to the control. Although the average surface air temperature anomalies are consistently positive throughout, for all space and time, with the largest values in the winter hemisphere at ice margins (see figure 2a), negative SST anomalies appear in the vicinity of the Irminger Sea and in the Weddell Sea. This pattern of local SST decrease (or much weaker increase than the rest of the ocean) is persistent throughout the entire experiment, with the largest decreases occurring in the Irminger Sea. This is the region in which the model produces most of its NADW in the control run. The result can be attributed to the suppressed production of deep water, and to a resultant reduction of the large convective heat flux from lower layers to the surface, which in the control run was responsible for the relatively warm temperatures in this region. The cooling process is accompanied by a freshening of surface waters in the North Atlantic and higher surface salinities at lower latitudes (figure 4).

A section through the western Atlantic (figure 5) shows the penetration of the warming signal into the deep ocean for the year 50. Except for polar regions, where the suppression of the upward deep convective heat flux is an efficient mechanism for warming the deep ocean, the warming is confined to the upper 1000 m. In the deep Atlantic, a cooling is seen. This is due to changes in the relative contribution of the different deep water sources, with an increased ratio in the production of cold, fresh AABW to warm, salty NADW.

The time evolution of the global mean sea level rise caused by thermal expansion is shown in figure 3c. In year 50 the global mean sea level rise is 19 cm. This is almost completely due to effects above the thermocline. The steady state sea level rise after 2000 years of integration is 51 cm. Whereas the prescribed atmospheric warming in year 50 has reached 72% of the equilibrium value, the response in global mean sea level is only 38.4%. Eighty years were required for the sea level to reach 50% of its equilibrium level, and 210 years to reach 75%. This clearly demonstrates the long time scales involved in the downward penetration of the

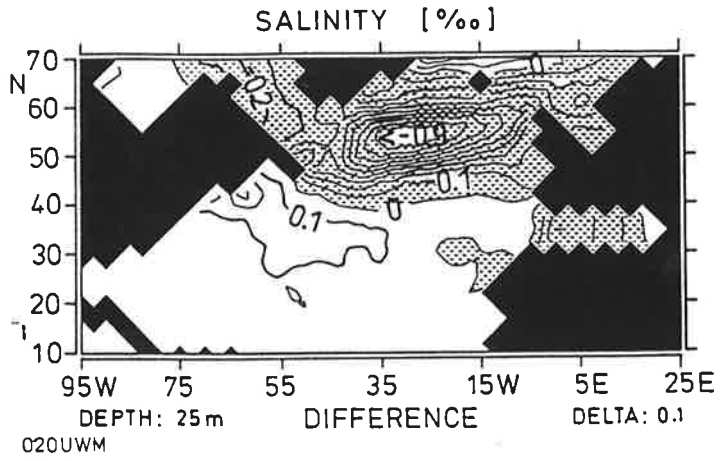

Figure 4: Geographical distribution of changes in the surface salinity in the North Atlantic in year 20 relative to the control experiment. Shading indicates negative values.

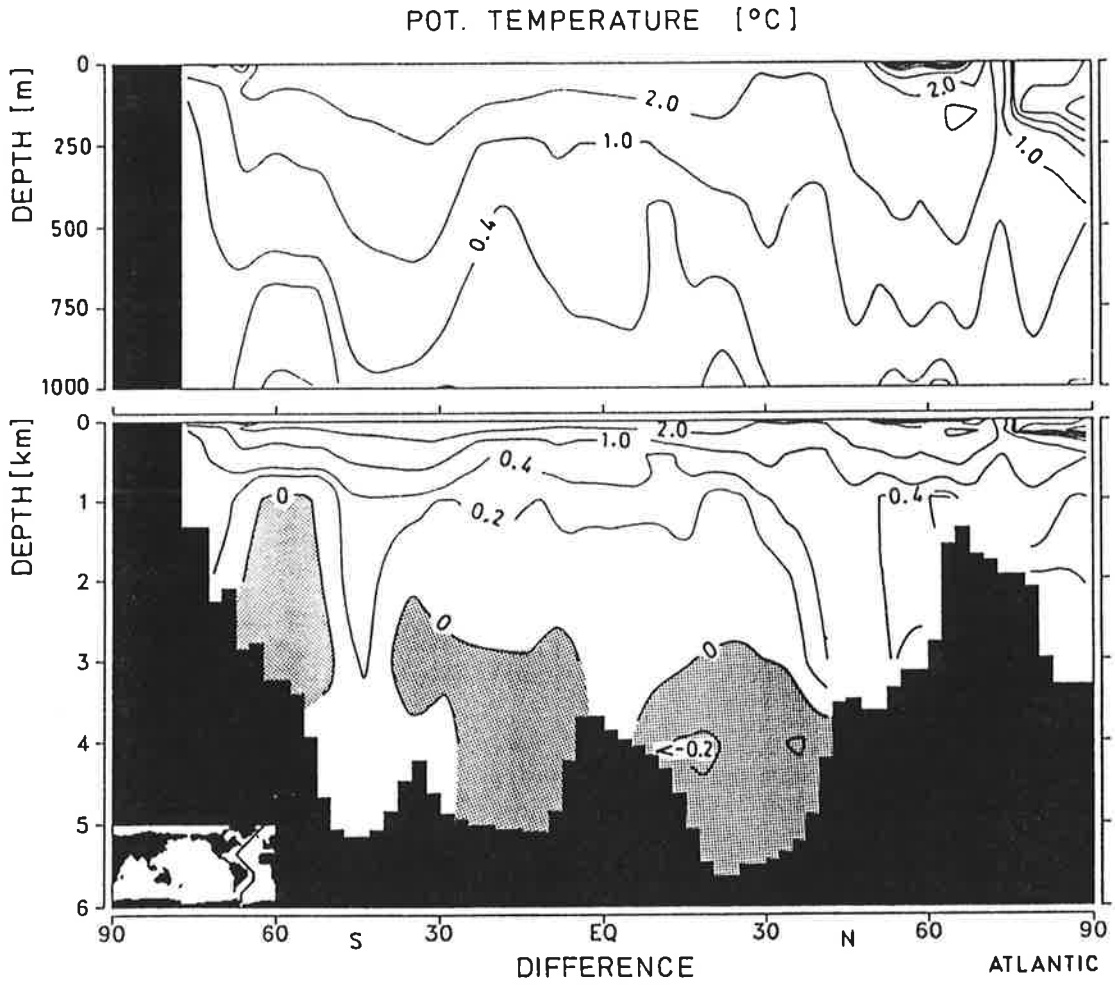

Figure 5: Pattern of change of potential temperature on a meridional section through the Atlantic in year 50 relative to the control experiment. The location of the section is shown in the insert. Shading indicates negative values.

warming signal.

The curves for selected locations differ considerably (figure 3c). The sea level increase of 35 cm in North-West Europe is almost twice as large as the global mean sea level change, while for example the increase in the Ross Sea is much smaller than the global mean. In general, the local sea level changes due to changes in the ocean circulation pattern are of the same magnitude as the changes due to the local thermal expansion, and both vary regionally.

The horizontal distribution of the sea level change for the year 50 is shown in figure 1b. The largest increases in sea level occur in the North Atlantic, as a result of the reduced NADW formation and reduced surface density, and on the northern edge of the ACC, through the southward displacement of the ACC. The increased gradient of sea level across the ACC is due to the larger fraction of bottom water produced at this location, as expressed by the increased vertical homogeneity of water mass properties.

5 Discussion

Coupled ocean-atmosphere models have not been used to investigate the sea level response to greenhouse-gas forcing (1,2,3). We are therefore restricted to comparing our sea level changes with results from simpler models.

Wigley and Raper (21) used an upwelling diffusive energy balance model to estimate the global sea level rise due to thermal expansion alone. For a comparable climate sensitivity ($\Delta T_{2x} = 4.5°C$) to that used here and "best guess" model parameters, they obtained an estimated global sea-level rise of 23 cm from 1985 to 2050. This is in good agreement with the global mean value obtained here (19 cm after 50 years).

With a simple model based on linear concepts of ventilation of the thermocline and Sverdrup balance, Godfrey et al.(6) arrived at a global sea level rise due to thermal expansion of between 13 and 30 cm after 60 years for an assumed global warming of 3°C in the first 40 years. This model also provides information on the spatial patterns of projected changes in sea-level. The authors obtain an almost uniform increase, with slightly weaker values around Antarctica. The disagreement with our results can be attributed to their neglect of changes in the deep water formation and the associated changes in the convective heat flux, which was found to be the most important effect in our experiment.

The circulation changes obtained here can be compared with those obtained in recent experiments with coupled ocean-atmosphere GCMs. A characteristic feature of our experiment, the cooling or reduced warming of SST in zones where deep water is produced, has been found also in a GFDL coupled AGCM-OGCM simulation with sector geography (1). The model's equilibrium response to CO_2-

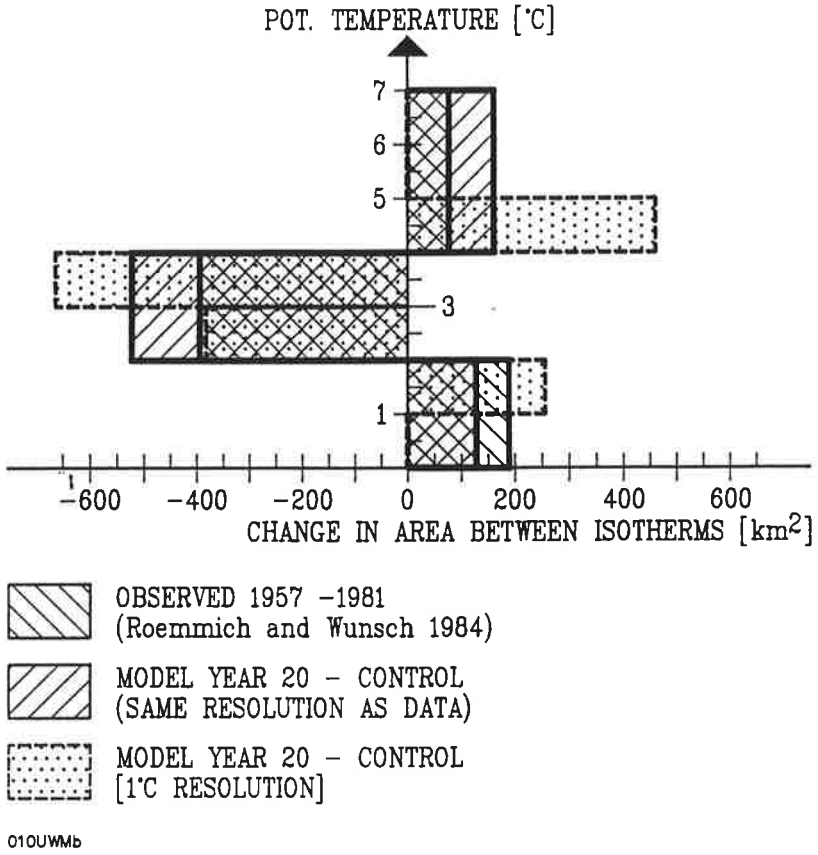

Figure 6: Observed vs. simulated relative changes in area between isotherms for a zonal Atlantic section at 24°N. In order to normalize the curves to the same bottom water temperature, 1°C has been subtracted from the model data. For the model results, two different resolutions have been plotted.

doubling yielded a cooling around Antarctica, with maxima located at the positions of strongest deep water formation in the control experiment. Due to an almost complete lack of NADW formation in this simulation, however, there was no equivalent cooling in the Northern Hemisphere.

The recent GFDL coupled AGCM-OGCM (3) simulation with a transient CO_2 increase of 1%/year (compound) shows similar results to those obtained in the present simulation. After 60 years of integration, the production of AABW is increased relative to NADW and in the zonal average a cooling is found in the deep ocean centered at 30° N (c.f. our figure 5). There is a relatively weak (compared to the zonal average) warming in the North Atlantic and a cooling around Antarctica. This pattern of SST changes generally corresponds to that obtained here, except for a discrepancy between our strong North Atlantic cooling and the weaker warming in the GFDL experiment. This discrepancy may be related to differences in the production of NADW, which is considerably weaker in the control run of the GFDL experiment than in our control run. The surface freshening which we obtain in the North Atlantic is also present in the GFDL simulation. The authors attribute this to a regional increase in runoff and precipitation minus evaporation, an explanation which cannot apply in our case.

The reduced production of NADW and the related cooling offers a possible explanation for the observed trend of decreasing marine air temperatures in the North Atlantic during the last 20 years, in contrast to the increase in Northern Hemisphere and Southern Hemisphere annually-averaged surface air temperature (22). Support for this conjecture is found in the observation of a strong negative salinity anomaly in the North Atlantic during the seventies. This anomaly was accompanied by suppression of convection and surface cooling (23). During this period the surface salinity further south (at ca. 40°N) was increased relative to the late fifties (24). A similar feature is found in the model response (figure 2b).

The simulated cooling in the deep Atlantic is consistent with the trend inferred from a comparison of temperature data taken in 1957 and 1981 for two transatlantic sections at 24°N and 36°N (25). Figure 6 shows the changes in areal coverage for observed (1981 minus 1957) and simulated (year 20 minus Control) isotherms for the section at 24°N. As the simulated deep water is roughly one degree warmer than the observations, the simulated curve has been reduced to the observed potential temperature in the bottom water by subtracting one degree from the simulated temperatures. The similarity between the two curves is striking.

However, although there are some striking similarities between the observed changes from the late fifties to the seventies and early eighties and the pattern which the model produces in response to the imposed warming, we stress that the observed anomalies could well be generated by other effects - for example, anomalous atmospheric circulation patterns (26). In the eighties the surface salinity in the North Atlantic was returning to its former values (23) and the relative cooling trend abated.

6 Conclusions

Significant changes are induced in the ocean circulation in response to an imposed forcing in surface air temperature corresponding to GCM equilibrium response results for a CO_2 doubling. In regions where deep water formation was formerly active, the projected increase in SST is small or even decreases relative to the zonal average. The formation of NADW is more strongly suppressed than the formation of AABW. The subsequent changes in deep water temperatures and salinities result in an effective cooling of the deep Atlantic. This signal may be useful in the detection of CO_2-induced climate change, although signal-to-noise problems are even more serious in the deep ocean than for surface data due to the sparseness of observations. Recently, the measurement of acoustic travel times has been proposed as a technique for monitoring deep ocean temperature changes associated with a CO_2 warming (27). The present experiment stresses the need for reliable ocean circulation response studies to compute the magnitude (and even sign!) of the expected temperature changes.

The projected atmospheric warming of ca. 3°C by the year 50 leads to a global sea level rise of 19 cm due to thermal expansion effects alone. Thermal expansion, however, is only one component of the simulated sea level response. Regionally-specific changes in the dynamic topography of the sea surface are of the same magnitude, with the strongest increases predicted in the North Atlantic, and the weakest increases (or even a decrease) predicted for the Ross Sea. Simpler models without a dynamic ocean cannot treat such effects in a realistic way. This shows the need for using an OGCM with realistic ocean circulation (particularly for the deep ocean) to simulate the regional sea-level changes in response to greenhouse-gas forcing.

The decrease in global deep water formation rates must be expected to have a strong impact on the atmospheric CO_2 content. At present, a significant fraction of the emitted CO_2 is transported with the newly-formed deep water to the deep ocean, thus limiting the increase in atmospheric pCO_2 (7). If the efficiency of this marine transport and storage mechanism is reduced, the increase in atmospheric pCO_2 will be amplified. This positive feedback can have important consequences for the evolution of future atmospheric pCO_2 concentrations.

Acknowledgements

Discussions with Klaus Hasselmann, Tom Wigley and Syd Levitus helped to improve this paper substantially. We gratefully acknowledge the assistance of Marion Grunert in preparing the diagrams.

References

1. Bryan, K., Manabe, S. and Spelman, M. J. *J. Phys. Oceanogr. 18*, 851-867 (1988).

2. Washington, W. and Meehl, G. *Clim. Dynamics 2*, 1-38 (1989).

3. Stouffer, R.J., Manabe, S. and Bryan, K. *Nature 342*, 660-662 (1989).

4. Gornitz, V., Lebedeff, S. and Hansen, J. *Science 215*, 1611-1614 (1982).

5. Wigley, T. M. L. and Raper, S. C. B. *Nature 330*, 127-131 (1987).

6. Godfrey, J. S., Church, J. A., Jackett, D. R. and McDougall, T. J. Submitted to *Nature*.

7. Maier-Reimer, E. and Hasselmann, K. *Clim. Dynamics 2*, 53-90 (1987).

8. Arakawa, A., Lamb, V. R. *Meth. Comp. Phys. 16*, 173-263 (1977).

9. Hellerman, S. and Rosenstein, M. *J. Phys. Oceanogr. 13*, 1093-1104 (1983).

10. Woodruff, S. D., Slutz, R. J., Jenne, R. L. and Steurer, P. M. *Bull. Am. Met. Soc. 68*, 1239-1250 (1987).

11. Levitus, S. Climatological Atlas of the World Ocean. *NOAA Professional Paper 13*, Rockville, Md. (1982).

12. Maier-Reimer,E. and Mikolajewicz, U. in *Oceanography 1988* (eds. Ayala-Castanares, A., Wooster, W. and Yanez-Arancibia) 87-100 UNAM-Press, Mexico D.F., 1990).

13. Roemmich, D. and Wunsch, C. *Deep-Sea Research 32*, 619-664 (1985).

14. Whitworth, T. and Peterson,R. G. *J. Phys. Oceanogr. 15*, 810-816 (1985).

15. Hansen, J., Lacis, A., Rind, D., Russell, G., Stone, P., Fung, I., Ruedy, R. and Lerner, J. in *Climate Processes and Climate Sensitivity* (eds Hansen, J. and Takahashi, T.), 130-163 (Am. Geophys. Union, Washington D.C., 1984).

16. Wetherald, R.T. and Manabe, S, *Clim. Change 8*, 5-23 (1986).

17. Schlesinger, M.E. and Zhao, Z.-C., *J. Climate* (in the press).

18. Wilson, C.A. and Mitchell, J.F.B. *J. Geophys. Res. 92*, 13315-13343 (1987).

19. Washington, W.M. and Meehl, G.A. *J. Geophys. Res. 89*, 9475-9503 (1984).

20. Hansen, J., Fung, I., Lacis, A., Rind, D., Lebedeff, S., Ruedy, R. and Russell,

G. *J. Geophys. Res. 93*, 9341-9364 (1988).

21. Wigley, T.M.L. and Raper, S.C.B. in *Climate and Sea Level Change: Observations, Projections and Implications* (eds. Warrick, R.A. and Wigley, T.M.L., 1990).

22. Jones, P.D., Wigley. T.M.L. and Farmer, G. in *Proceedings of DOE Workshop on Greenhouse-Gas-Induced Climatic Change* (ed M.E. Schlesinger; in the press, 1990).

23. Dickson, R. R., Meincke, J., Malmberg, S.-A. and Lee, A. J. *Progr. Oceanogr.* 20, 103-151 (1988).

24. Levitus, S. *J. Geophys. Res. 94*, 9679-9685 (1989).

25. Roemmich, D. and Wunsch, C. *Nature 307*, 446-450 (1984).

26. Dickson, R. R., Lamb, H. H., Malmberg, S.-A. and Colebrook, J. M. *ICES, Contribution to Council Meetings 1984 Gen 4* (1984).

27. Munk, W. H. and Forbes, A. M. G. *J. Phys. Oceanogr. 19*, 1765-1778, 1989.